

Dynamical Phase Transitions In Driven Integrate-And-Fire Neurons

Jan R. Engelbrecht¹ and Renato Mirolo²

¹*Department of Physics, Boston College, Chestnut Hill, MA 02467 and*

²*Department of Mathematics, Boston College, Chestnut Hill, MA 02467*

We explore the dynamics of an integrate-and-fire neuron with an oscillatory stimulus. The frustration due to the competition between the neuron's natural firing period and that of the oscillatory rhythm, leads to a rich structure of asymptotic phase locking patterns and ordering dynamics. The phase transitions between these states can be classified as either tangent or discontinuous bifurcations, each with its own characteristic scaling laws. The discontinuous bifurcations exhibit a new kind of phase transition that may be viewed as intermediate between continuous and first order, while tangent bifurcations behave like continuous transitions with a diverging coherence scale.

Neurons in awake, behaving mammals receive complicated dendritic input currents and respond with highly irregular trains of action potentials. Unraveling the meaning of each neuron's train of spikes is a formidable challenge. A simple starting point is to characterize a neuron's activity in terms of its firing rate (which varies in time in behaving organisms), or in terms of temporal correlations between its spike times and that of other neurons, either individually or collectively in a local rhythm. There is a long history of detecting rhythmic neural activity at various scales, from electroencephalography (EEG), to local field potentials, to oscillatory membrane currents stimulating individual pyramidal and interneurons in voltage clamp recordings.

In this letter we present a biophysical approach to explore consequences of rhythmic inputs on the rate and timing of a model neuron's spikes. Our framework is directly relevant for describing the behavior of a neuron in a slice preparation with blocked dendritic inputs and controlled injection of a simple stimulus current in a whole-cell patch-clamp setting. Our analysis may also shed light on the time scales and (transient) dynamical patterns in the spike trains that may develop for the more complicated stimuli neurons receive in vivo. Advocating a statistical-mechanical perspective, where minimal models yield insight into universal behavior of more realistic models, we consider the one-dimensional integrate-and-fire (IF) model[1]. An IF model neuron receiving a constant current stimulus has a constant firing rate. We consider the consequences of an additional small oscillatory input; this second, competing time scale introduces frustration that results in pattern formation. We explore connections between these stable patterns and the description of critical phenomena associated with continuous phase transitions.

The IF model describes the response of a cell's membrane potential $v(t)$ to an influx of current I . The voltage evolves according to the differential equation $\tau(dv/dt) = -(v - v_{eq}) + RI$, together with the condition that when $v(t)$ reaches a threshold v_{th} , an instantaneous action potential is generated and $v(t)$ is reset to an equilibrium resting potential v_{eq} . We use units where R is the membrane resistance and the time constant $\tau = RC$ is proportional to the membrane capacitance C . The parameters R , I , τ , v_{eq} and v_{th} are all time-independent. We set $\Delta v = v_{th} - v_{eq}$ and assume throughout that $\Delta v > 0$. If we start with an initial condition $v(t_0) = v_{eq}$, then the potential $v(t)$ will always reach threshold provided $RI > \Delta v$. In this case the neuron fires at a con-

stant rate, with interspike interval $T_{nat} = -\tau \log(1 - \Delta v / RI)$.

Next we consider the effect of adding a secondary periodic stimulus current $E \cos \omega t$, which introduces a competing time scale $T_{drv} = 2\pi/\omega$. The governing equation is now

$$\tau \frac{dv}{dt} = -(v - v_{eq}) + RI + E \cos \omega t. \quad (1)$$

We view the rhythm $E \cos \omega t$ as a perturbation of the constant current term, and in this spirit limit our attention to the case $0 \leq E < RI$. The introduction of a second, competing time scale leads to a loss of the simple periodic behavior of the original model. As we shall see, the model neuron typically no longer has a constant interspike interval, and can exhibit both periodic and aperiodic firing patterns.

We again start with $v(t_0) = v_{eq}$ (changing t_0 allows us in effect to adjust the relative phase of the cosine drive at the initial condition). The next spike time t_1 is the first solution to $v(t) = v_{th}$ with $t > t_0$; a solution exists provided $RI + E/\sqrt{(\omega\tau)^2 + 1} > \Delta v$. The dependence of t_1 on t_0 determines a return map F ; iterating the map F generates a spike train $t_0 < t_1 < t_2 \dots$ via $t_n = F(t_{n-1}) = F^n(t_0)$.

The map F is continuous when

$$RI \geq E + \Delta v \quad (2)$$

(this implies $\dot{v} > 0$ for $v < v_{th}$) and is discontinuous otherwise. The source of this discontinuity is illustrated in Fig. 1, which shows solutions to (1) with nearly identical initial conditions in the two different cases where condition (2) is satisfied (green) and not satisfied (red). When (2) fails (1) has a solution with $\dot{v} = 0$ at threshold, which causes a jump discontinuity in the return map F .

We are interested in the evolution of the interspike intervals (ISIs) $t_n - t_{n-1}$ for $E > 0$, especially whether these

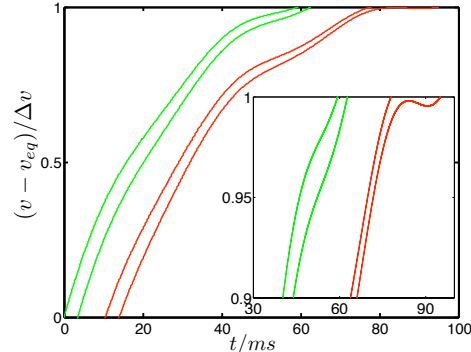


FIG. 1: Solutions to (1) when (2) holds (green) and fails (red).

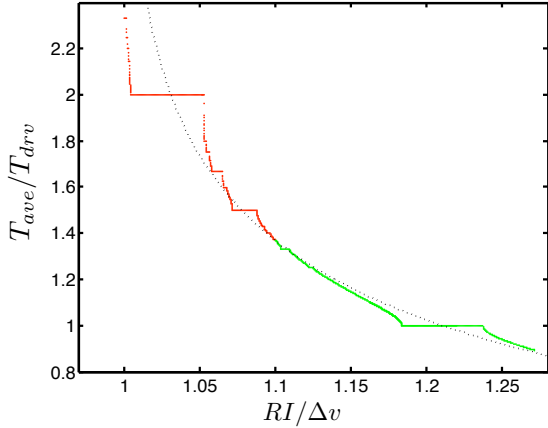


FIG. 2: Average period in units of the drive period vs. the parameter RI for drive amplitude $E = 0.1\Delta v$, $\tau = 20ms$ and $T_{drv} = 35ms$. The dotted curve is T_{nat}/T_{drv} , which is proportional to the period in the undriven case.

intervals become periodic and if so, how rapidly such a pattern is established. The asymptotic dynamics are determined by the average interspike interval

$$T_{ave} = \lim_{n \rightarrow \infty} \frac{t_n}{n} = \lim_{n \rightarrow \infty} \frac{F^n(t_0)}{n} \quad (3)$$

i.e., the inverse of the neuron's firing rate.

The map F satisfies the periodicity relation $F(t + T_{drv}) = F(t) + T_{drv}$ reflecting the periodicity of the drive term. Consequently, from the theory of circle maps [2, 3, 4], the limit defining T_{ave} exists, is independent of the initial condition t_0 and depends continuously on the parameters (RI , τ , ω and E). Furthermore, the dimensionless ratio T_{ave}/T_{drv} is a rational number $r = p/q$ iff

$$F^q(t^*) = t^* + p T_{drv} \quad (4)$$

for some t^* ; in other words t^* is a fixed point of the map $F^q(t) - p T_{drv}$. So the spike train beginning with $t_0 = t^*$ satisfies $t_{n+q} = t_n + pT_{drv}$ and consequently the sequence of phases of t_n relative to T_{drv} repeats every q firings.

In Fig. 2 we plot T_{ave}/T_{drv} as a function of the parameter RI , while keeping fixed $T_{drv} = 35ms$, $\tau = 20ms$ and $E = 0.1\Delta v$. We divide the graph into two regions according to whether the return map is continuous (green) or discontinuous (red). For a given number r , let RI_r^- and RI_r^+ denote the minimum and maximum values of RI for which $T_{ave}/T_{drv} = r$. $RI_r^- < RI_r^+$ iff r is a rational number; in other words the plateaux in Fig. 2 correspond to rational multiples of the drive period. When r is an integer and the return map is continuous (green part), RI_r^\pm can be determined algebraically; in this special case

$$RI_r^\pm = \frac{\Delta v}{1 - e^{-2\pi\tau/\omega\tau}} \pm \frac{E}{\sqrt{(\omega\tau)^2 + 1}}, \quad (5)$$

and $T_{ave} = T_{nat}$ at the midpoint of the plateau. The width of such a plateau is then proportional to E , the magnitude of the oscillatory drive. In all other cases, RI_r^\pm needs to be determined numerically.

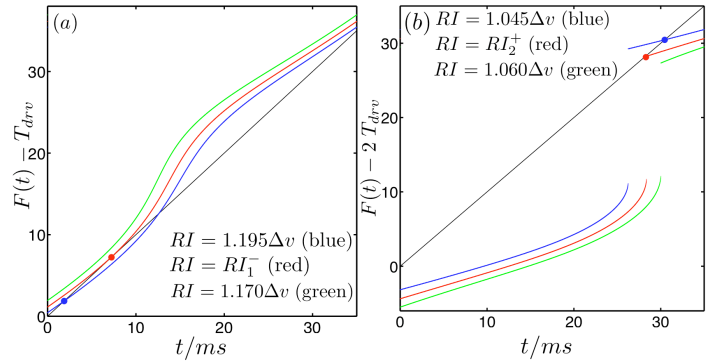


FIG. 3: (a) Return maps associated with the tangent bifurcation at left edge of the $r = 1$ plateau; (b) Return maps associated with the discontinuous bifurcation at right edge of the $r = 2$ plateau.

The asymptotic structure of the average firing rate as in Fig. 2 has been known for some time[3, 4, 5]. In this paper our focus is on *the approach* to the asymptotic behavior, and the resulting connection to dynamical *phase transitions*. The circle map theorem[2] guarantees that the asymptotic value of T_{ave} for a given RI is independent of the initial condition t_0 . This stability allows us to view Fig. 2 as a phase diagram, with each plateau a state corresponding to some rational number r which we express as a fraction $r = p/q$ (in lowest terms). These states are analogous to phases of matter and the boundaries of the plateaux to phase transitions.

Within each p/q entrainment plateau, the spike train converges to a periodic pattern of ISI's that repeats every q spikes, corresponding to a stable fixed point of $F^q(t) - pT_{drv}$. For perfect p/q entrainment $t_{n+q} - t_n - pT_{drv} = 0$; hence

$$\Delta_n^{p,q} = t_{n+q} - t_n - pT_{drv} \quad (6)$$

measures the deviation from p/q entrainment. The convergence (within a plateau) is geometric, so $\Delta_n^{p,q} \sim x^{-n}$.

Henceforth we fix τ , ω and E and consider the parametric dependence on RI . The fixed points of $F^q(t) - pT_{drv}$ vary with RI and ultimately vanish through some kind of bifurcation at the edges of the p/q entrainment plateau. Analogous to the theory of phase transitions, the equation

$$\Delta_n^{p,q} \sim e^{-n/\xi_\tau(RI)} \quad (7)$$

defines a coherence time $\xi_\tau(RI)$ that characterizes how rapidly the phase-locked solution is approached. Of particular interest is how $\xi_\tau(RI)$ scales with respect to the tuning parameter RI as an edge of an entrainment plateau (phase boundary) is approached. As we shall show, the scaling has a universal form dictated by the type of bifurcation through which the fixed points are lost.

We first analyze the phase transitions and associated scaling behaviors that occur in the parameter range when the return map F is continuous, as in Fig. 3(a). Upon varying RI the fixed point is here lost through a *tangent* bifurcation. The generic behavior near such a phase boundary is modeled by the simple map $g(x) = x - x^2 + \lambda$, which has a stable fixed point at $x^* = \sqrt{\lambda}$ that is lost through a tangent bifurcation as the control parameter $\lambda \rightarrow 0$. Let $\delta x_n = x_n - x^*$; then $\delta x_{n+1} - \delta x_n = -2\sqrt{\lambda} \delta x_n - (\delta x_n)^2$, which has large n solution $\delta x_n \sim \exp(-2\sqrt{\lambda} n)$ so $x_n \rightarrow x^*$ with a coherence time

$\xi \sim 1/\sqrt{\lambda}$. This generic scaling holds for each fixed point of $F^q(t) - pT_{drv}$ and as the phase boundary is approached from within a plateau the coherence time then scales as

$$\xi_\tau(RI) \sim \frac{1}{|RI - RI_r^\pm|^{\frac{1}{2}}} \quad (8)$$

consistent with classical exponent $\nu = \frac{1}{2}$ in equilibrium critical phenomena[6].

The coherence time diverges at the phase boundary (when the control parameter $RI = RI_r^\pm$), and the dynamics can again be modeled by the map $g(x)$. In this case $\lambda = 0$, the fixed point $x^* = 0$ and the δx_n^2 term above becomes relevant. The large n solution is now $x_n \sim 1/n$ and hence $x_{n+1} - x_n \sim -1/n^2$; in particular the fixed point at the tangent bifurcation is no longer approached geometrically. Analogously, the p/q -entrainment coherence at the phase boundary then develops according to the power law

$$\Delta_n^{p,q} \sim \frac{1}{n^2} \quad (9)$$

consistent with a critical exponent $\eta = 0$.

As we vary the control parameter RI so as to exit the p/q entrainment plateau, ‘‘bottlenecks’’ develop near the locations of the q lost fixed points. The resulting dynamics can again be modeled by the map $g(x)$ which has a bottleneck near $x = 0$ for small negative λ . As $\lambda \rightarrow 0^-$, the number of iterations N_λ needed to pass through a fixed interval $[-c, c]$ around zero scales like $N_\lambda \sim 1/\sqrt{|\lambda|}$. N_λ characterizes how long it takes to pass through a single bottleneck and introduces a time-scale outside the entrainment plateau that diverges similar to the coherence time in eqn. (8).

The approach to p/q entrainment is illustrated in Fig. 4 which demonstrates exponentially fast coherence of the form (7) inside the 1-1-plateau, the power-law form (9) at the phase boundary and bottleneck behavior just outside the 1-1-entrainment phase. The repeated bottleneck behavior represents failed entrainment to this particular p/q -entrainment phase. If this pattern eventually repeats periodically, the average period will converge to different rational multiple of T_{drv} and hence lie on a different p'/q' -entrainment plateau; otherwise T_{ave}/T_{drv} is irrational.

For RI just outside the plateau, the deviation of the average period from rT_{drv} is inversely proportional to the number of iterations required to pass through the bottleneck caused by lost fixed point of $F^q(t) - pT_{drv}$; thus

$$|T_{ave} - rT_{drv}| \sim |RI - RI_r^\pm|^{\frac{1}{2}}. \quad (10)$$

This average deviation of entrainment plays the role of a disorder parameter which, in analogy to equilibrium phase transitions, identifies the exponent $\beta = \frac{1}{2}$. This scaling form is illustrated in Fig. 5.

Generically, a smooth map F can acquire or lose periodic points only through tangent bifurcations, which dictate the universal scaling near the phase boundaries described above. However, when the map is discontinuous it can also acquire or lose periodic points through a *discontinuous* bifurcation. As we shall see, the associated scaling near the phase boundaries for these bifurcations belongs to a new universality class.

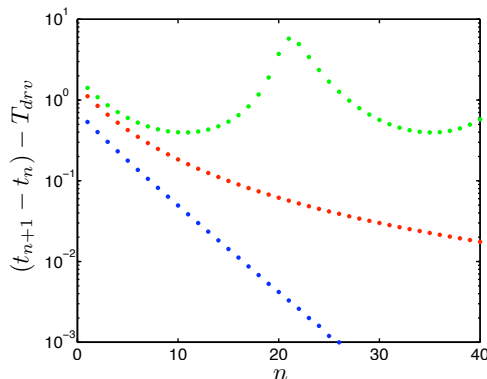


FIG. 4: Approach to entrainment in ISI’s ($\Delta_n^{1,1}$) inside (green), at (blue) and outside (red) the left edge of the 1/1 plateau, respectively exhibiting scaling of (7), (9) and bottleneck behavior.

An example of this type of bifurcation is illustrated in Fig. 3(b), for $r = 2$. The behavior at the bifurcation (phase boundary) depicted here differs fundamentally from the continuous case in Fig. 3(a), in that the slope of the map at the fixed point here remains strictly less than one. Consequently, iterates of the map still converge to the fixed point following the geometric form in (7), corresponding to a finite coherence time at the bifurcation, as opposed to power law scaling.

To explore the behavior near the plateau edges for discontinuous bifurcations, we introduce a simple map h of the form $h(x) = ax + \lambda$ for $x > 0$ (with $0 < a < 1$) and with a discontinuous jump at $x = 0$. As λ sweeps through zero, the fixed point of $h(x)$ is lost in a bifurcation similar to that seen in Fig. 3(b). Since the map is linear for $x > 0$, successive iterations satisfy $x_n = h^n(x_0) = x^* + a^n(x_0 - x^*)$ while $x_n > 0$, where $x^* = \lambda/(1 - a)$ which is a fixed point of $h(x)$ for $\lambda > 0$. A bottleneck near $x = 0$ again develops for λ small negative, and even though $x^* < 0$ is then not a fixed point of $h(x)$, it still controls the passage through the bottleneck in terms of the expression for x_n above. The number of iterations N_λ needed to pass through an interval $[0, c]$ is determined by solving $0 = h^n(c)$ for n (and rounding up to the nearest integer). As $\lambda \rightarrow 0^-$, the solution scales like $N_\lambda \sim -\ln|\lambda|$.

Consequently, for RI just outside the edge of a plateau at which a discontinuous bifurcation occurs, the deviation of the average period from rT_{drv} scales as

$$|T_{ave} - rT_{drv}| \sim \frac{-1}{\ln|RI - RI_r^\pm|}. \quad (11)$$

So our disorder parameter vanishes *logarithmically* at phase boundaries determined by discontinuous bifurcations, slower than any power law.

Note that the functions F graphed in Fig. 3(b) are increasing and have slope $+\infty$ on the left at the discontinuities. Furthermore, the dependence of F on the parameter RI is such that as RI increases, the graph of F moves downward. These properties hold in general for all maps F maps under consideration as well as the iterates F^q . At a bifurcation the map $F^q(t) - pT_{drv}$ still has fixed points but must also lie completely on one side of the line $y = t$. The bifurcation is discontinuous if these fixed points occur at the disconti-

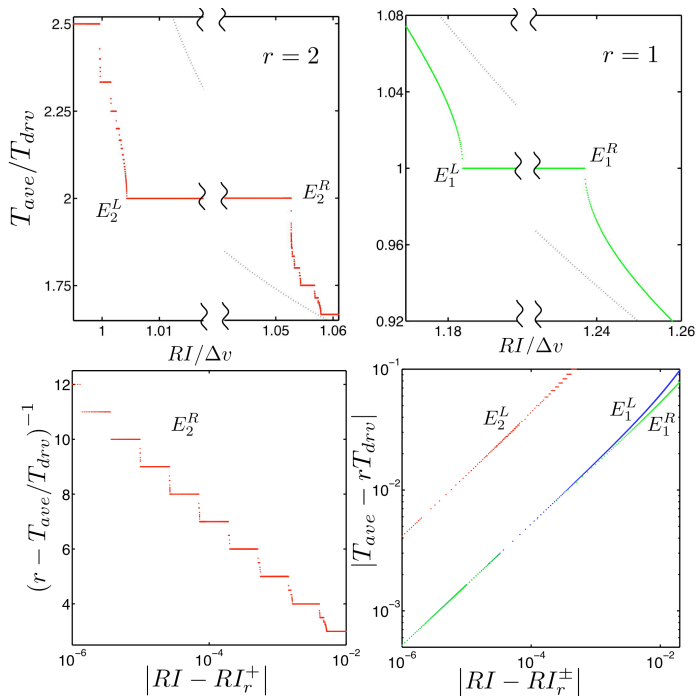


FIG. 5: Scaling in T_{ave} near the edges of the $r = 2$ and $r = 1$ plateaux. Edge E_2^R demonstrates the logarithmic scaling in (11) at a discontinuous bifurcation, while edges E_2^L , E_1^L and E_1^R exhibit power law scaling in (10) at tangent bifurcations.

nities of the map. Since F^q has slope $+\infty$ on the left at the jump discontinuities, the fixed points at a discontinuous bifurcation must occur on the right side of the jump discontinuities, and the map $F^q(t) - pT_{drv}$ must lie *below* the line $y = t$. These fixed points are lost upon increasing RI and consequently discontinuous bifurcations can only occur on the right edges of the plateaux, as is the case in the particular example illustrated above for $r = 2$. In other words, the bifurcations occurring at the left edges of the entrainment plateaux are all tangent bifurcations, even in the parameter range where F is discontinuous.

On the other hand, both types of bifurcations occur at the right edges in the parameter range where F is discontinuous, although tangent bifurcations are quite rare. For example, in Fig. 2 tangent bifurcations occur at the right edges of the plateaux for $r = \frac{3}{2}$, $\frac{7}{5}$ and $\frac{11}{8}$; all the other right-edge bifurcations we investigated in this parameter range are discontinuous. Furthermore, in this example, the bifurcations at the right edges are *all* discontinuous for RI below some threshold. In fact, we can show that such a threshold exists if the oscillatory drive E is sufficiently small relative to Δv (technically when $E < \Delta v / (1 + ((\omega\tau)^2 + 1)^{-\frac{1}{2}})$). The point is that under this condition, the map F is concave up every-

where for RI sufficiently small and since F is increasing, the same holds for all its iterates. This rules out the possibility of tangent bifurcations at right edges of plateaux; i.e., where the map $F^q(t) - pT_{drv}$ is below the line $y = t$.

In conclusion, periodically driven IF neurons lose p - q entrainment through two markedly different routes, corresponding to the tangent and discontinuous bifurcations described above. Each has its own characteristic universal scaling laws which measure the rate of convergence to entrainment within the p - q plateau as well as the deviation from p - q entrainment just outside the plateau.

In equilibrium statistical mechanics, a phase transition is classified as either *continuous*, which has a diverging coherence scale (ξ) and a vanishing order parameter at its critical point, or *first order*, which has no diverging coherence scale and a discontinuous jump in the order parameter at its transition. The scaling laws at tangent bifurcations are identical to that of a continuous phase transition with ‘classical’ exponents $\beta = \frac{1}{2}$, $\nu = \frac{1}{2}$ and $\eta = 0$. However, the behavior at the discontinuous bifurcations does not match our conventional understanding of phase transitions with universal scaling. The finite coherence time at the discontinuous bifurcations is a feature of first order phase transitions, which have discontinuous jumps in their order parameters and no universal scaling laws. But as we have seen, T_{ave} varies continuously and hence the disorder parameter $T_{ave} - rT_{drv}$ vanishes at the bifurcation, as is the case for continuous phase transitions. The logarithmic scaling law for $T_{ave} - rT_{drv}$ vanishes more slowly than any power law, and hence exhibits behavior which is intermediate between conventional continuous and first order phase transitions.

For conventional continuous phase transitions, universal scaling results from the singularity associated with a diverging coherence scale. Our discontinuous bifurcation does not have such a diverging scale, yet exhibits a new kind of universal scaling. Here it is the singularity in the discontinuous map that is responsible for universality.

From a neuro-physiological perspective, our results suggest that when a neuron firing with some rate receives an additional rhythmic stimulus, a range of p - q entrainment possibilities exist. Moreover, the convergence to entrainment to a p - q phase-locked firing pattern is characterized by a coherence time which depends sensitively on the distance to the entrainment plateau edge. Whole-cell slice recording, where an individual cell is stimulated with a constant plus oscillatory current injection, would be an ideal setting in which to explore in vitro the scaling and pattern formation discussed in this letter.

JRE acknowledges very useful conversations with John Hopfield and David Sherrington and support from ICAM.

[1] P. Dayan and L. F. Abbott, *Theoretical Neuroscience*, MIT Press (2001).
 [2] R. L. Devaney, *An Introduction to Chaotic Dynamical Systems*, Addison Wesley (1989).
 [3] B. W. Knight, *Jnl. Gen. Physiol.*, **59** (1972) 734.
 [4] J. P. Keener, *Trans. Amer. Math. Soc.*, **261** (1980) 589.

[5] J. P. Keener, F. C. Hoppenstead and J. Rinzel, *SIAM J. Appl. Math.*, **41** (1981) 503.
 [6] N. Goldenfeld, *Lectures on Phase Transitions and the Renormalization Group*, Addison-Wesley, 1992.